JOURNAL OF NEUROTRAUMA 37:55–65 (January 1, 2020)

DOI: 10.1089/neu.2019.6485

Dynamic Thermal Mapping of Localized Therapeutic Hypothermia in the Brain

John J. Walsh,[1] Yuegao Huang,[2] John W. Simmons,[3] James A. Goodrich,[4] Brian McHugh,[5,6] Douglas L. Rothman,[1,2] John A. Elefteriades,[7] Fahmeed Hyder,[1,2] and Daniel Coman[2]

Abstract

Although whole body cooling is used widely to provide therapeutic hypothermia for the brain, there are undesirable clinical side effects. Selective brain cooling may allow for rapid and controllable neuroprotection while mitigating these undesirable side effects. We evaluated an innovative cerebrospinal fluid (CSF) cooling platform that utilizes chilled saline pumped through surgically implanted intraventricular catheters to induce hypothermia. Magnetic resonance thermal imaging of the healthy sheep brain ($n=4$) at 7.0T provided dynamic temperature measurements from the whole brain. Global brain temperature was 38.5 ± 0.8°C at baseline (body temperature of 39.2 ± 0.4°C), and decreased by 3.1 ± 0.3°C over ~30 min of cooling ($p<0.0001$). Significant cooling was achieved in all defined regions across both the ipsilateral and contralateral hemispheres relative to catheter placement. On cooling cessation, global brain temperature increased by 3.1 ± 0.2°C over ~20 min ($p<0.0001$). Rapid and synchronized temperature fall/rise on cooling onset/offset was observed reproducibly with rates ranging from 0.06–0.21°C/min, where rewarming was faster than cooling ($p<0.0001$) signifying the importance of thermoregulation in the brain. Although core regions (including the subcortex, midbrain, olfactory tract, temporal lobe, occipital lobe, and parahippocampal cortex) had slightly warmer (~0.2°C) baseline temperatures, after cooling, temperatures reached the same level as the non-core regions (35.6 ± 0.2°C), indicating the cooling effectiveness of the CSF-based cooling device. In summary, CSF-based intraventricular cooling reliably reduces temperature in all identified brain regions to levels known to be neuroprotective, while maintaining overall systemic normothermia. Dynamic thermal mapping provides high spatiotemporal temperature measurements that can aid in optimizing selective neuroprotective protocols.

Keywords: brain; MRS; selective cooling; temperature mapping; therapeutic hypothermia

Introduction

In traumatic brain injury (TBI) and its concomitant ischemic injury, the promise of neuroprotection from therapeutic hypothermia remains elusive. The rapid and timely delivery of therapeutic hypothermia for patients with TBI remains problematic. Two recent randomized clinical trials (RCT)—EuroTherm 3235 and POLAR-RCT—failed to show a treatment effect of therapeutic hypothermia for TBI.[1,2] Unlike patients with cardiac arrest or neonatal hypoxic-ischemic encephalopathy, where the timely application of hypothermia provides neuroprotection, patients with brain injury present a complex array of conditions and comorbidities that hinder early application of prophylactic hypothermia.

Another potential confounding variable may relate to the method of hypothermia delivery itself. In many previous studies, including the two large randomized trials, the primary methodology to induce hypothermia was the use of intravenous solutions or endovascular devices to achieve systemic whole body cooling. Here we evaluate an innovative technology to induce localized hypothermia in the brain to temperatures known to be neuroprotective, while maintaining overall systemic (i.e., body) normothermia.

Physical and ischemic brain injuries result in inflammatory processes and dysregulated brain cooling mechanisms leading to brain temperatures higher than measured core body temperatures.[3] Therefore, decreasing the brain temperature (therapeutic hypothermia) has been shown to be neuroprotective. Therapeutic hypothermia has demonstrated efficacy and has become a mainstay in management of global cerebral ischemia after cardiac arrest, with further evidence suggesting a neuroprotective benefit after TBI and

[1]Department of Biomedical Engineering, [2]Department of Radiology and Biomedical Imaging, [4]Department of Comparative Medicine, [5]Department of Neurosurgery, [7]Aortic Institute, Yale University, New Haven, Connecticut.
[3]CoolSpine LLC, Woodbury, Connecticut.
[6]Inova Medical Group Neurosurgery, Fairfax, Virginia.

ischemic stroke. Together, these conditions represent major contributors to morbidity and mortality in the United States.[4]

Despite hundreds of unsatisfying pharmacological attempts to identify drugs with neuroprotective effects, hypothermia remains a viable therapeutic option that has demonstrated efficacy. Experimental studies in animal models of ischemic stroke have shown a clear benefit of hypothermia in reducing infarct volumes. Moreover, hypothermia in animal models of TBI has demonstrated neuroprotective effects.[5]

Cerebral temperatures are approximated easily in the absence of pathology when brain and body temperatures are similar and regulated by the hypothalamus. In pathological states, however, brain temperature may deviate from body temperatures.[6] In addition, under anesthesia, brain temperature decreases.[7,8] Temperatures are elevated in ischemic stroke lesions in the brain,[9] and after brain injury, temperature is usually higher than in normal states. The greatest benefit of hypothermia is achieved in the period immediately after the physical or ischemic injury, and it is therefore critical to start treatment immediately at symptom/trauma onset. The neuroprotective effects may be lost if hypothermia is induced after reperfusion.

Brain temperature is coupled closely to brain metabolism/perfusion, and tight temperature control is critical for normal brain function.[3] In animals, changes in brain temperature of 2–3°C have been observed with behavioral stimuli, providing a link between increased brain metabolism/activity and temperature. There is a close relationship between temperature and oxidative metabolism, which is a measure of brain activity.[10] Although temperature is increased in hypermetabolic states, thermoregulatory effects can compensate to lower brain temperature. Because heat exchange in the brain is hindered by its location within the insulating skull, heat is removed primarily by an increase in blood flow. Cerebral flow-metabolism coupling may be lost during hypothermia, where decreased temperature leads to a decrease in both metabolism and blood flow.[3]

Although whole body cooling strategies have been proposed and tested, significant side effects limit their use. These include shivering, decrements in cardiovascular function, immunosuppression leading to higher rates of infection and pneumonia, ion/electrolyte imbalances, and problems with coagulation and acid/base regulation.[11] For ischemia, such as after cardiac arrest, where many organ systems are affected, whole body cooling is likely beneficial. For brain injury or focal ischemia during stroke, however, targeted brain cooling may be more advantageous by limiting systemic adverse effects. Despite the obvious need for techniques that selectively cool the brain, and possibly even only cool the single affected hemisphere, few current options are available.

The challenge in achieving this aim is to develop techniques that can be implemented quickly in a clinical setting during the critical time window immediately after the injury or onset of ischemia and before reperfusion injury. Methods to lower temperatures can be either non-invasive or invasive.[12,13] Non-invasive methods rely on cold packs/blankets, which generally lower core body temperature as well as brain temperature, or pharyngeal cooling, which may be more selective but is limited to temperature decreases of 1–3°C.[14,15] To alleviate these effects, invasive methods try to directly cool the brain. This has been achieved using endovascular approaches whereby intravenous or intraarterial catheters have been inserted and used for intravascular injections of cooled saline/blood.[16]

While providing direct and selective cooling, these methods result in transient cooling and are limited by the volume of solution that may be infused, limiting the magnitude of the temperature decrease and the duration of the effect. Depending on catheter placement, these techniques can result in more specific cooling of the brain with less impact on body temperature.

Here we utilize a novel cerebrospinal fluid (CSF)-cooling based platform that allows for chilled saline to be pumped through a closed-loop catheter inserted into the lateral ventricles of the brain.[17] The refrigerant enters by one lumen of the catheter and exits by another, never interacting directly with the CSF. This novel system cools the CSF conductively and, via natural CSF flow, allows convective cooling of the entire brain. Invasive strategies generally are used to provide selective cooling to the brain in an effort to reduce the side effects associated with systemic whole-body cooling. While there are added risks with invasive procedures, this method provides rapid, direct, and reversible cooling that can be maintained over an extended period.

To demonstrate the efficacy of intracerebral cooling is challenging, given the location of the brain beneath the skull. Further, regional measurements of variations in temperature within the brain, although usually lacking, indeed are required to understand the neuroprotective effects of hypothermia—for example, when particular brain regions are not being cooled effectively. Although there are both intraparenchymal and intraventricular temperature probes for monitoring brain temperature directly, these methods allow only for localized temperature measurements at the precise site of the temperature probe. Dynamic and more comprehensive measurements of temperature distributions during cooling are necessary to understand the cooling efficiency of any cooling device before clinical translation.

To achieve this, we have used a magnetic resonance spectroscopic imaging (MRSI) method called Biosensor Imaging of Redundant Deviation in Shifts (BIRDS), which uses the temperature-dependent chemical shifts of paramagnetic lanthanide-based macrocyclic contrast agents, such as $TmDOTMA^-$, to yield quantitative, high-resolution temperature measurements across the entire brain.[18,19]

Using BIRDS, we measured the temperature maps in four healthy sheep brains before, during, and after the onset of cooling induced by the implanted CSF cooling device. The results show sustained decreases in brain temperature across both hemispheres at the onset of cooling, with a return to baseline temperatures after the cessation of cooling. Throughout all experiments, systemic normothermia of the animals was maintained. Thus, temperature mapping with BIRDS provided a direct measurement of cooling efficiency of the CSF cooling device, which can be further employed in evaluating selective brain cooling strategies for therapeutic hypothermia.

Methods

Four juvenile crossbreed neutered male sheep (*Ovis aries*) weighing 26.5 and 24.2 kg (age: 14 weeks), 34.5 and 32.0 kg (age: 22 weeks) were supplied by Thomas D. Morris, Inc. (Reisterstown, MD). The lambs were pair housed, provided with environmental enrichment, and acclimated in the Yale Animal Resource Center for 9–10 days before surgery and imaging procedures. The room temperature was maintained at 22.2 ± 1.1°C with a photoperiod of 12 h of light and 12 h of darkness. Water and hay were provided *ad libitum,* and animals were fed 2–3% of body weight daily with commercially prepared ruminant diet (Teklad 7060) supplemented with fresh vegetables. Each animal was examined and determined to be healthy and free of clinical disease by Yale veterinary clinicians.

The Animal Care program is fully accredited by the Association for the Assessment and Accreditation for Laboratory Animal Care

International (AAALAC), and all procedures and experiments were approved in advance by the Yale University Institutional Animal Care and Use committee (IACUC).

Each fasted lamb was premedicated with acepromazine (0.05 mg/kg) dosed intramuscularly and then induced with ketamine (2.7 mg/kg) and diazepam (0.2 mg/kg) intravenously to allow endotracheal intubation and subsequent maintenance on isoflurane gas (1–3%) via mechanical ventilation. Buprenorphine (0.01 mg/kg) was given intramuscularly to provide opioid analgesia and lactated Ringers solution was administered intravenously at the continuous rate of 4 mL/kg/h for fluid maintenance. Thermal support was provided with a circulating warm water pad to control and maintain body temperature (38–39°C), and an orogastric tube was placed to allow venting of gas, thus preventing excessive rumen distension.

Before the initial incision, a local anesthetic injection of 0.5% bupivacaine solution (1 mg/kg) was made at the surgery site to provide multimodal analgesia. Continuous monitoring of the depth of anesthesia and stability of vital signs in the surgery suite was accomplished using a Mindray DPM6 patient monitor (Mindray DS USA, Inc). Burr holes were made bilaterally 1.5 cm anterior and lateral to the posterior fontanelle at an angle of 10 degrees from the sagittal plane on each side. A pediatric slotted stylet was inserted through each burr hole and guided anatomically into the lateral ventricle. Proper location in the lateral ventricle was confirmed by CSF flow, and pressures were measured by manometry.

The cooling catheters were designed by CoolSpine, LLC (Woodbury, CT) and contain three lumens: two lumens accomplish the delivery and removal of supersaturated saline in a closed loop circuit, which is maintained at -7 to -10°C. In addition, the third lumen functions as an external ventricular drain for intracranial pressure management. This lumen was modified to allow contrast agent infusion during the imaging procedures. $TmDOTMA^-$ (7 mg/kg) was infused directly into the lateral ventricles at an infusion rate of 1 mL/h. Two cooling catheters were placed via the burr holes directly into both the right and left lateral ventricles (named right and left catheters, respectively). This technique is consistent with capabilities of common clinical practice in neurological intensive care units. Continuous monitoring of the depth of anesthesia and vital signs in the magnetic resonance imaging (MRI) suite was accomplished using an Invivo Precess 3160DCU patient monitor (Invivo Corporation Orlando, FL). After the completion of the imaging procedures, each animal was euthanized with an intravenous dose of sodium pentobarbital-based euthanasia solution (Euthasol®).

The MRI and spectroscopy (MRS) datasets were obtained on a Varian 7.0T/68 cm horizontal-bore spectrometer (Magnex Scientific Ltd.) using a ^1H resonator/surface coil RF probe. The MR images were acquired using a 128×128 gradient-echo (GE) pulse sequence with a field of view (FOV) of $10\,cm \times 10\,cm$, with 17 slices of 5 mm thickness with a repetition time (TR) of 200 msec and an echo-time (TE) of 5 msec. The $17 \times 17 \times 17$ three-dimensional (3D) chemical shift imaging (CSI) datasets were acquired with spherical encoding of k-space as described previously[20] with a TR of 20 msec and a FOV of $15.3\,cm \times 15.3\,cm \times 15.3\,cm$. A single-banded refocused 90-degree Shinnar-Le Roux radiofrequency pulse of 40 kHz bandwidth and 500 μsec was used for selective excitation of the $TmDOTMA^-$ methyl group protons.

The CSI data were reconstructed to $34 \times 34 \times 17$ resolution with a voxel size of $4.5 \times 4.5 \times 9.0\,mm^3$. The spectra were line broadened (200 Hz), phased (zero order), and baseline corrected (first order) in Matlab. The temperature was calculated in each voxel from the chemical shift of $TmDOTMA^-$ methyl group $\boldsymbol{\delta_{CH3}}$ according to the equation:

$$T = a_1 + a_2(\delta_{CH3} + 103) + a_3(\delta_{CH3} + 103)^2 \quad (1)$$

where δ_{CH3} is the measured chemical shift of the methyl resonance of $TmDOTMA^-$ and a_1, a_2, and a_3 are 34.45 ± 0.01, 1.460 ± 0.003, and 0.0152 ± 0.0009, respectively, from linear least square fitting of calibration data over the physiological range of temperature values.[19] The temperature from each voxel was measured and plotted in an axial slice, which was coregistered with anatomical imaging to show the spatial distribution of the temperature values throughout the brain.

During the imaging session, baseline anatomical images were acquired before the $TmDOTMA^-$ infusion. Next, baseline temperature maps were acquired to establish the basal brain temperature. Then the flow of cooling solution was started through the right catheter at a rate of 35 mL/min, during which CSI data for temperature mapping were obtained. Each animal underwent a cooling paradigm with temperature maps acquired at 10 min intervals throughout all phases of cooling and recovery.

In two animals, flow was initiated in the right catheter, and after cooling for 40 min, flow was then directed through both catheters with increasing flow rates up to 48 mL/h before cooling was stopped and the temperature was allowed to recover. In two additional animals, flow was initiated in the right catheter for 30 min and then stopped for 10 min to allow the temperature to recover. The flow was then restarted in only the left catheter for 30 min. Again after a cooling period, the flow was either stopped and the temperature was allowed to recover or flow was initiated through both catheters.

Throughout all phases of cooling and recovery, CSI data were obtained every 10 min for temperature mapping. A final CSI dataset for temperature mapping was obtained at the end of the experiments after the cessation of cooling to show the return of temperature toward normothermia.

For consistency of the analysis when calculating cooling or recovery rates, we used temperature measurements obtained during the first cooling event in each sheep. The initial cooling phase was considered to be the period after the baseline temperature mapping and until the first period of recovery (during which the flow through the catheter had been stopped). Similarly, the initial recovery phase was the first period during which flow through the catheter was stopped, but before flow of the cooling solution was restarted. The rate of temperature change k was calculated based on the change in temperature (ΔT) divided by the time interval over which the change occurred (Δt).

$$k = \frac{\Delta T}{\Delta t} \quad (2)$$

The subsequent diverse time courses of temperature change in individual animals (when flow was initiated either through each catheter or when flow was increased through both catheters) were used to show the robustness and reproducibility of the cooling technique.

Regional variations of temperature were assessed by assigning voxels to regions of interest (ROIs) corresponding to different brain regions based on a previously published high-resolution sheep brain atlas.[21] All statistics were performed based on average ROI temperature values. All temperature measurements, changes in temperature, and rates of change of temperature are all reported as mean ± standard deviation. All comparisons were assessed using a two-tailed *t* test where p values <0.05 were considered to be significant.

Results

MRI of catheter placement

Four sheep underwent catheter placement in both the right and left lateral ventricles. Gross anatomy of the sheep brain provides landmarks that were used for identification of morphological features and for registration to imaging datasets (Fig. 1A). The intraventricular catheter (Fig. 1B) is composed of a tube with a distensible sac at the end to allow variable expansion according to the available ventricle volume and shape. The catheter was designed to circulate

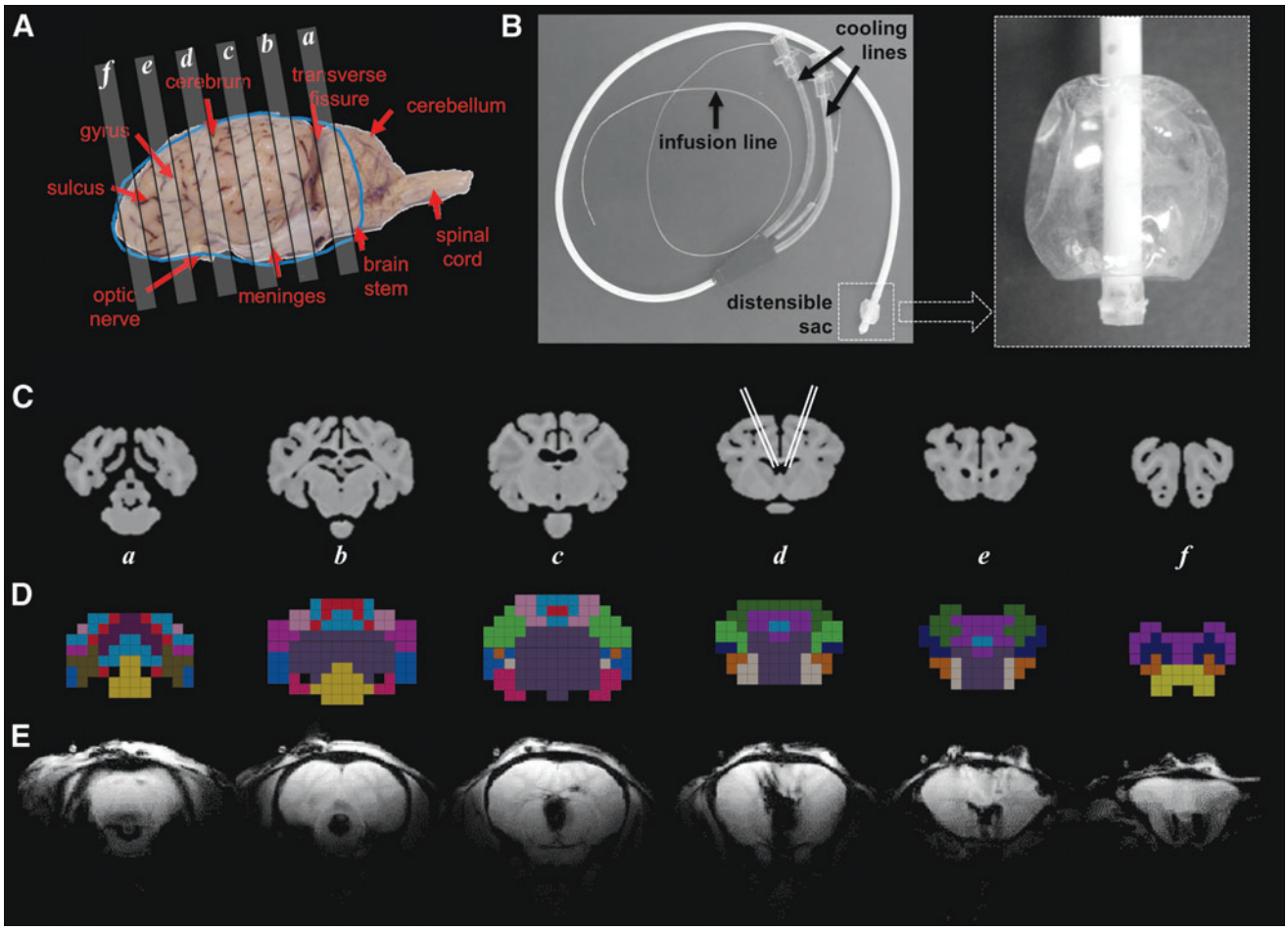

FIG. 1. Representative anatomical images of the sheep brain and description of the cooling device. The gross anatomy of the sheep brain (**A**) is shown with several axial slices identified. The cooling catheter used for intraventricular cooling (**B**) was inserted at an angle into the lateral ventricles of both hemispheres. Representative high-resolution anatomical magnetic resonance (MR) images corresponding to axial slices in (A) are shown in (**C**), along with the approximate location of the catheters in slice d (Adapted with permission from *Journal of Comparative Neurology*, 2017, 525, 676–692). Using a previously published anatomical atlas,[21] a lower resolution CSI-based anatomical atlas was generated, and 17 distinct regions of the brain were identified and color-coded (**D**). The region identifications are summarized in Supplementary Figure 1; see online supplementary material at www.liebertpub.com. The MR images acquired during the temperature studies (**E**) were used for localization of various brain regions.

chilled saline in a closed circuit via two cooling lines, one for inflow and the other for outflow, to and from the distensible sac. A third (central) line was used for release of the CSF pressure created by the expansion of the distensible sac during cooling. The contrast agent was infused via a thin delivery line (P10) positioned inside the central (pressure-release) line (Fig. 1B).

A previously published high resolution anatomical atlas of the sheep brain (Fig. 1C) was used to group its 53 high resolution brain regions[21] into 17 separate larger brain regions (Fig. 1D and Supplementary Fig. 1; see online supplementary material at www.liebertpub.com), that were used subsequently for regional temperature mapping analysis. The regrouping of some of the smaller anatomical regions into larger ones was necessary for better overlap with the lower resolution (4.5 mm × 4.5 mm × 9 mm) CSI grid.

The numbering of the regions used here is the same as that used in the high-resolution anatomical atlas. Some of the small regions in the high-resolution anatomical atlas, however, were combined in the CSI atlas, reducing the number of regions from 53 to 17. Therefore, the numbering of the regions is not continuous because, when several regions were combined into one, the combined region was named using the number of the largest original region. The T_2-weighted anatomical images of the sheep brain were used to verify the approximate position of catheter placement (Fig. 1E).

Temperature mapping

BIRDS was used successfully for 3D temperature mapping of sheep brain after administration of $TmDOTMA^-$ at a resolution of $4.5 \times 4.5 \times 9.0\,mm^3$, acquired in about 10 min and repeated throughout several cooling and recovery processes for each animal (Fig. 2). The temperature was calculated according to equation 1. Average baseline temperature in the sheep brain was $38.5 \pm 0.8°C$, with corresponding body temperature of $39.2 \pm 0.4°C$. We used a sagittal slice through the center of the brain to show the temperature distribution in the sheep brain (Fig. 2A) pre-cooling, post-cooling, and after recovery, corresponding to distinct time points in the temperature time course (Fig. 2B, marked with #, *, and $, respectively).

For all animals, three independent BIRDS measurements were made to establish a baseline temperature before cooling. After chilled saline began to be circulated in the catheters, temperature

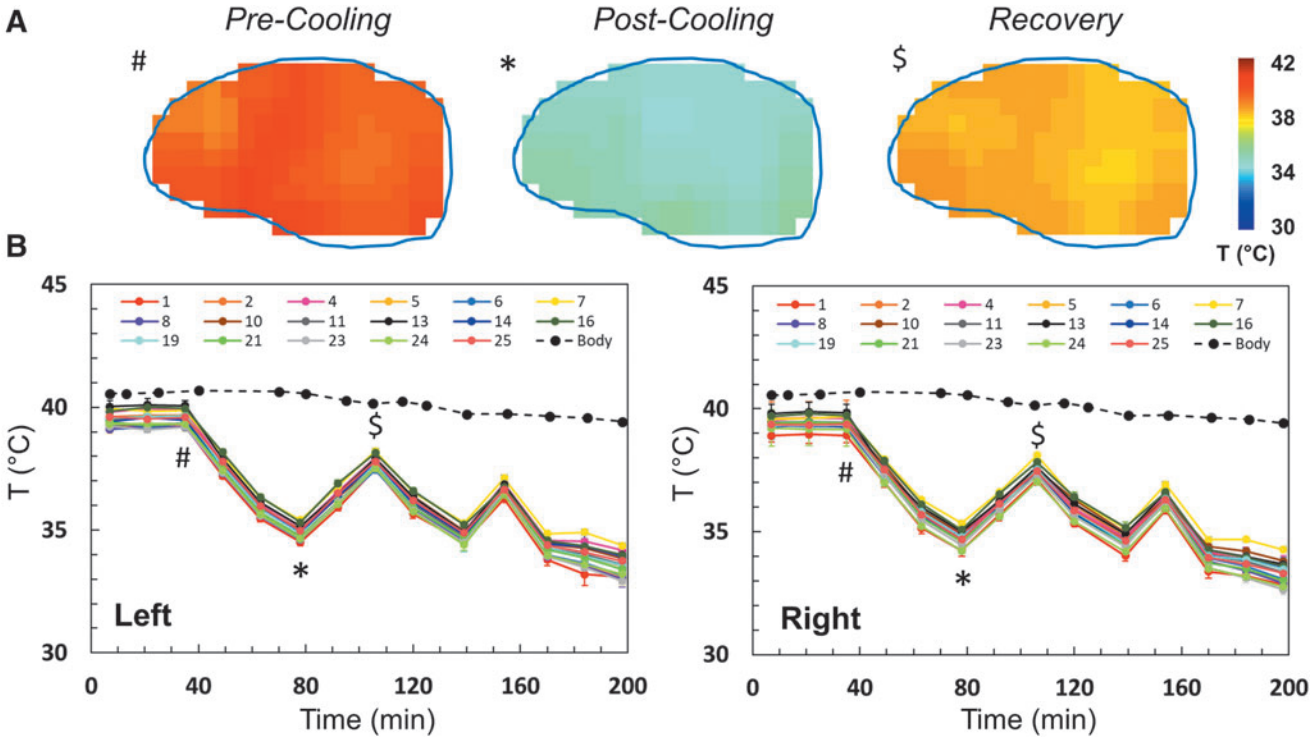

FIG. 2. Representative example of temperature variation during intraventricular cooling in a sheep brain. During the experiment, several baseline temperature maps were obtained. Temperature maps were then acquired every 10 min during repeated cooling and recovery cycles, using catheters lateralized to a single hemisphere or in both hemispheres. At the end of the experiment, the flow rate of the chilled saline through the catheter was increased from 35 to 42 mL/min to show that further temperature reductions could be achieved. Temperature maps of a central sagittal slice before cooling (#), after cooling (*), and after recovery ($) are shown in (**A**). The corresponding time points are indicated using the same symbols on the temperature versus time curve in (**B**). The average temperature over time in each of the 17 anatomically defined regions was calculated (B). In addition, the core body temperature was also measured throughout the duration of the experiment and is shown for comparison. The time course shown represents sheep 4 as shown in Figure 4 and Figure 5.

measurements using BIRDS continued throughout the duration of the experiment. Separate measurements of the left and right hemispheres (Fig. 2B) are shown for each of the 17 brain regions investigated. The time course for temperature in all four animals shows reproducible temperature changes throughout the cooling and recovery process (Supplementary Fig. 2; see online supplementary material at www.liebertpub.com).

Although brain temperature fluctuated rapidly with the onset/offset of cooling, body temperature remained nearly constant and normothermic throughout the duration of the experiment (Fig. 2B). The water bath temperature used to maintain the body temperature in the anesthetized animals was not adjusted throughout the experiment, such that the temperature fluctuation represents maintenance of body temperature despite thermal support.

Global brain temperatures were measured as an average of all temperature measurements over the entire brain (Table 1). An average 11% decrease (4.2°C) in brain temperature was observed in the four sheep, while the brain temperature decreased an average of

Table 1. Temperature Results for Each Sheep

	Core body temp (CBT, °C)	*Baseline brain temp (BBT, °C)*	*Nadir brain temp (NBT, °C)*	*% Decrease CBT vs. NBT*	*% Decrease BBT vs. NBT*	p *value*
Sheep 1	38.9 ± 0.3	37.6 ± 0.2	33.9 ± 0.4	12.8	9.8	$p < 0.00001$
Sheep 2	38.2 ± 0.5	38.3 ± 0.2	33.8 ± 0.2	11.4	11.7	$p < 0.00001$
Sheep 3	38.5 ± 0.2	38.7 ± 0.2	35.7 ± 0.2	7.4	7.9	$p < 0.00001$
Sheep 4	39.9 ± 0.7	39.5 ± 0.3	33.4 ± 0.4	16.3	15.3	$p < 0.00001$
Mean	38.9 ± 0.8	38.5 ± 0.7	34.2 ± 0.9	12.0	11.2	$p < 0.00001$

Core body temperatures are calculated as an average of all values before initiation of cooling. Baseline brain temperatures are calculated as global brain temperatures just before initiation of cooling. Nadir brain temperatures represent the lowest global brain temperatures reached throughout cooling. Percent changes in temperature are calculated relative to both core body temperature and baseline brain temperatures. All values are reported as mean ± standard deviation. Statistical analyses are performed using a two-tailed Student *t* test with *p* values <0.05 considered significant.

12% relative to core body temperature. The results of the temperature measurements pre- and post-cooling and after recovery in the 17 regions are shown for the left (Fig. 3A) and right (Fig. 3B) brain hemispheres. The differences in baseline temperatures between all regions were distributed throughout a 0.7°C range.

Moreover, based on anatomical identification of brain regions using the high-resolution sheep brain atlas, the 17 brain regions were combined further into two main regions: one superficial (termed non-core) and one deep (termed core) (Supplementary Fig. 3; see online supplementary material at www.liebertpub.com). We employed this two-zone separation to better understand the differences between superficial and deeper brain structures.

The core contained the regions identified as the subcortex, midbrain, olfactory tract, temporal lobe, occipital lobe, and parahippocampal cortex. The rest of the 17 regions were combined into a non-core (superficial) region. When grouped by core and non-core regions, the results show non-significant temperature differences ($p > 0.05$) between left and right brain hemispheres in both core and non-core regions, pre- and post-cooling and after recovery (Fig. 3C). Post-cooling temperatures reached 35.5 ± 0.6°C vs. 35.6 ± 0.2°C in the right and left hemispheres of the brain, respectively, showing no differences relative to catheter placement (Fig. 3C).

When left and right hemispheres were analyzed together (Fig. 3D), the pre-cooling (baseline) temperature of the core of the brain was slightly warmer than non-core regions (~ 0.2°C) but was not significant ($p = 0.26$). Post-cooling, average brain temperature (including both core and non-core regions) decreased significantly ($p < 0.0001$, 38.5 ± 0.7°C vs. 35.6 ± 0.6°C) and after recovery temperatures increased significantly ($p < 0.0001$, 35.6 ± 0.6°C vs. 37.6 ± 0.4°C). No significant differences were found between core and non-core regions.

Interestingly, the temperature after cooling did not differ significantly throughout the different regions of the brain. Although there were slight differences in basal temperatures between core and non-core regions of the brain, the initially warmer core regions reached the same temperature after cooling as the non-core regions, reflecting greater cooling efficiency of the core regions of the brain (Fig. 3C, 3D).

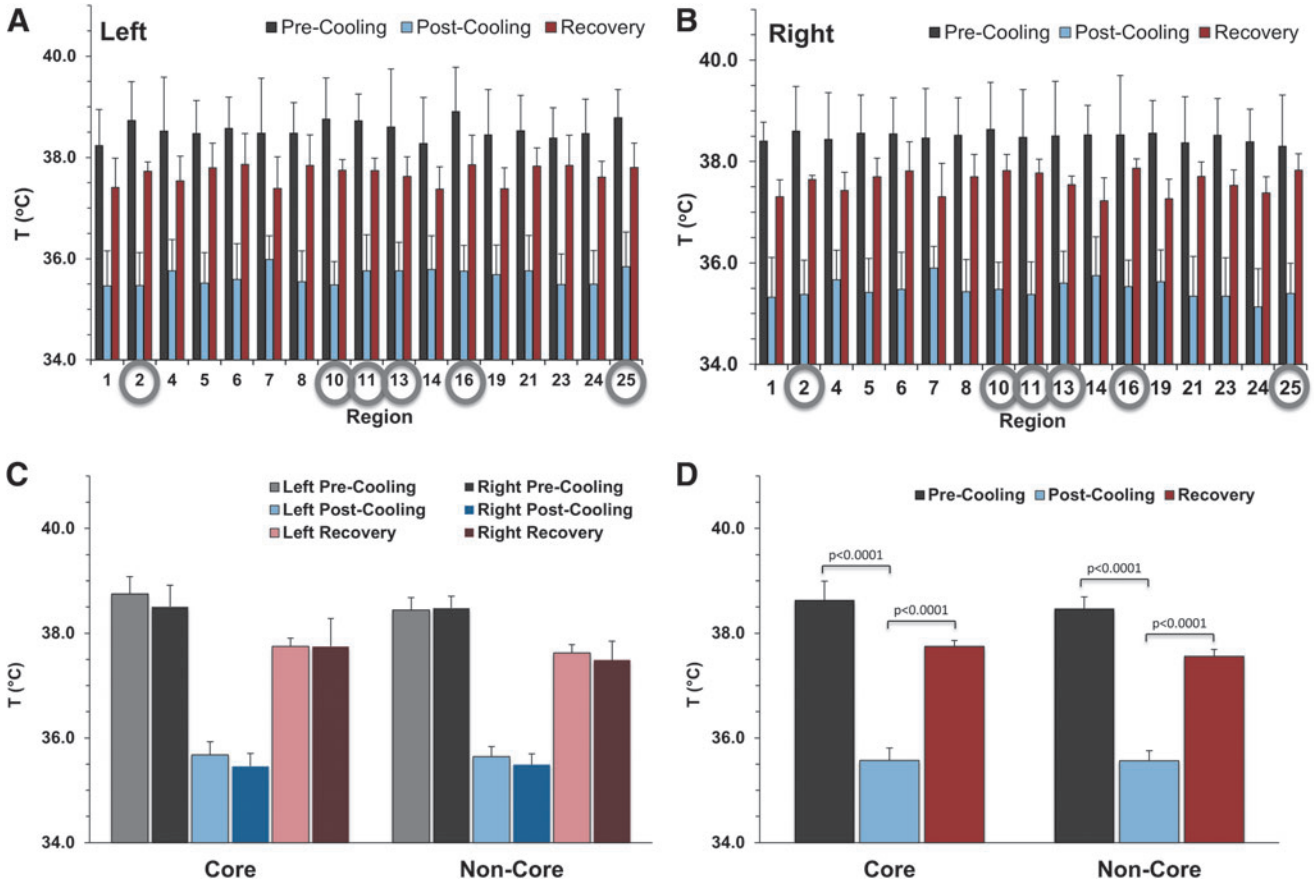

FIG. 3. Absolute temperature measurements from various regions of the brain averaged across all animals. The pre- and post-cooling and the recovery temperatures are reported for the 17 brain regions (shown in Supplementary Figure 1) as average ± standard deviation in the left (**A**) and right (**B**) hemispheres. Based on their location, these 17 brain regions were combined further into core (deep) and non-core (superficial) regions (Supplementary Figure 3). The core regions (subcortex, midbrain, occipital lobe, olfactory tract, parahippocampal cortex, and temporal lobe) are identified by gray circles in (A) and (B), while the rest are the non-core regions. The average temperature in the left and right hemispheres for the core and non-core regions is reported before cooling, after cooling, and after recovery (**C**). No significant changes are observed between the right and left hemisphere of the brain. Average temperatures across the entire brain (**D**) are also shown. In all regions and for the entire brain, statistically significant temperature decreases ($p < 0.0001$) were achieved during cooling with corresponding significant temperature increases ($p < 0.0001$) after recovery.

Temperature changes and rates of change during cooling and recovery

To further quantify the efficiency of cooling, regional variations in the magnitude of temperature change and the rate of change in temperature throughout the brain were calculated. For consistency, we calculated the temperature changes and the corresponding cooling rates only during the first cooling event, done in each of the four sheep using the catheter positioned in the right ventricle. Similarly, we calculated the temperature changes during recovery and the corresponding recovering rates only during the first recovery event.

Cooling using one intraventricular catheter resulted in a rapid temperature decrease throughout both core and non-core regions in each sheep (Fig. 4A). Similar temperature changes during cooling were also measured in both the left and right hemispheres (light vs. dark colors in Fig. 4C, 4D). Post-cooling, the absolute temperature throughout the brain was significantly lower, with changes in the range from -2.1°C (in the non-core region of sheep 2, Fig. 4C) to -4.7°C (in the core region of sheep 4, Fig. 4C).

When averaging the measurements in all four sheep, temperature changes of -3.2 ± 0.5°C and -3.1 ± 0.5°C were observed in the core of the left and right hemispheres, respectively (Fig. 4D). In the non-core regions of the brain, the average temperature changes were -2.9 ± 0.4°C and -3.1 ± 0.4°C for the left and right hemispheres, respectively (Fig. 4D). Although slightly greater temperature decreases were observed in core vs. non-core regions of the brain (~0.2°C), this was not found to be significant ($p = 0.43$, Fig. 4D).

During the recovery period, the temperature in the core regions of the brain increased to a greater extent than in the non-core regions (Fig. 4B, 4C, 4D). In the core regions, the average temperature changes during recovery were 3.4 ± 0.3°C and 3.3 ± 0.4°C for the left and right hemispheres, respectively, while in the non-core regions, these were 3.0 ± 0.2°C and 2.9 ± 0.2°C (Fig. 4D). Although there were no significant differences between the left and right hemispheres, there was a greater temperature change (0.4°C) observed in the core regions versus non-core regions ($p = 0.01$, Fig. 4D). The measured temperatures after recovery showed a reestablished temperature gradient in the brain, with core regions slightly warmer than the non-core regions (37.8 ± 0.1°C vs. 37.6 ± 0.1°C, Fig. 3D).

To further investigate how fast the brain is cooled, the rate of temperature change (equation 2) was compared between core and non-core regions of the brain. Synchronized temperature fall/rise on

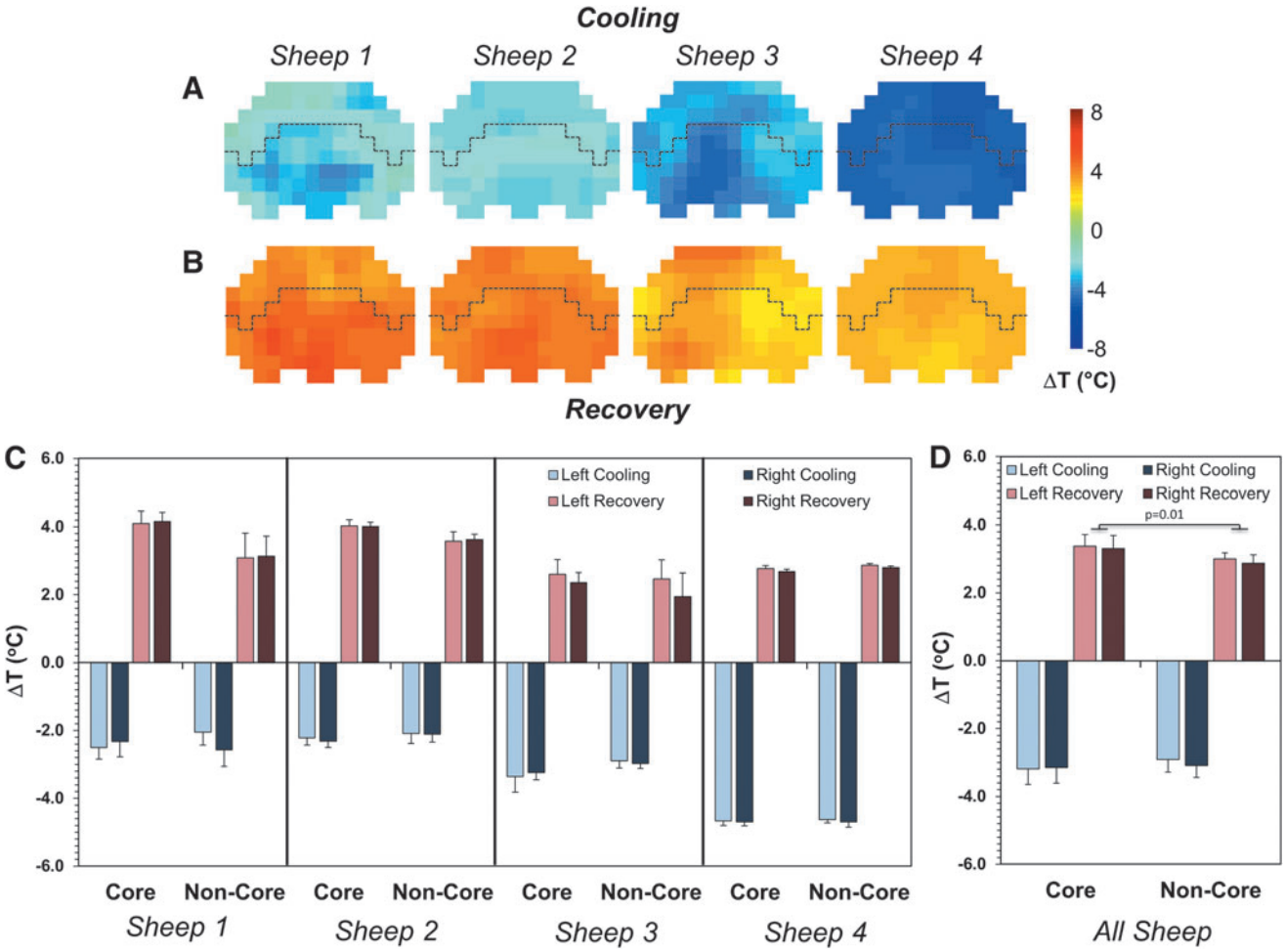

FIG. 4. Temperature changes during cooling and recovery in all four sheep. Spatial distributions of the absolute temperature change in an axial slice (slice c in Fig. 1) during the first cooling event using the right catheter (**A**) and during the first recovery (**B**). Quantification of the absolute change in temperature during cooling and recovery are shown for both the left and right hemispheres for core and non-core regions of the brain in individual animals (**C**). Average absolute temperature changes are reported for all animals (**D**) with significant differences ($p = 0.01$) between core and non-core regions of the brain during recovery. Temperature changes are all reported as average ± standard deviation. The dashed line in (A) and (B) represents the demarcation between the core (bottom) and non-core (top) regions.

cooling onset/offset was observed with cooling rates ranging from 0.05 to 0.11°C/min and recovery rates ranging from 0.06 to 0.21°C/min (Fig. 5A, 5B). Cooling rates were identical between core and non-core regions, but slightly faster (but not significant) rates were detected during rewarming in core regions ($p = 0.18$, Fig. 5C, 5D). There were no differences, however, between ipsilateral or contralateral hemispheres of the brain relative to catheter placement.

The average cooling rates were -0.082 ± 0.009°C/min and -0.080 ± 0.010°C/min in the core of the left and right hemispheres, respectively, while in the non-core regions, the rates were -0.074 ± 0.024°C/min and -0.079 ± 0.026°C/min (Fig. 5D). The average recovery rates were 0.118 ± 0.024°C/min and 0.116 ± 0.026°C/min in the core and 0.103 ± 0.012°C/min and 0.100 ± 0.014°C/min in the non-core regions of the left and right hemispheres, respectively (Fig. 5D).

We also examined whether the volume of the ROI had an effect on the absolute temperature changes and on the rates of cooling/recovery. The subcortex was the largest ROI used in the analysis (volume: 12 mL), while there were many ROIs with smaller volumes (1–3 mL, Supplementary Fig. 1; see online supplementary material at www.liebertpub.com). The results show that not only the temperature changes during both cooling and recovery (Supplementary Fig. 4A, 4B; see online supplementary material at www.liebertpub.com), but also that the cooling and recovery rates (Supplementary Fig. 4C, 4D) were independent of the size of the various brain structures being cooled.

Further temperature decrease was achieved either when we cooled using both catheters or when we increased the flow rate of the circulating chilled saline (Supplementary Fig. 2; see online supplementary material at www.liebertpub.com). When cooling the brain using both catheters, we achieved an additional temperature decrease of 1.7 ± 0.5°C in the contralateral (left) hemisphere, and 1.2 ± 0.3°C in the ipsilateral (right) hemisphere (sheep 1 and 2, Supplementary Fig. 2). Moreover, after we increased the flow rate through both catheters from 35 to 42 mL/min, we achieved another additional temperature decrease of 0.9 ± 0.3°C in the contralateral (left) hemisphere, and 1.0 ± 0.4°C in the ipsilateral (right) hemisphere (sheep 2 and 4, Supplementary Fig. 2).

The maximum temperature decrease observed was 6.5 ± 0.1°C measured in several gyrus regions (ectolateralis, lateral, posterior sylvian, suprasylvius, and sylvian) in the right hemisphere in sheep

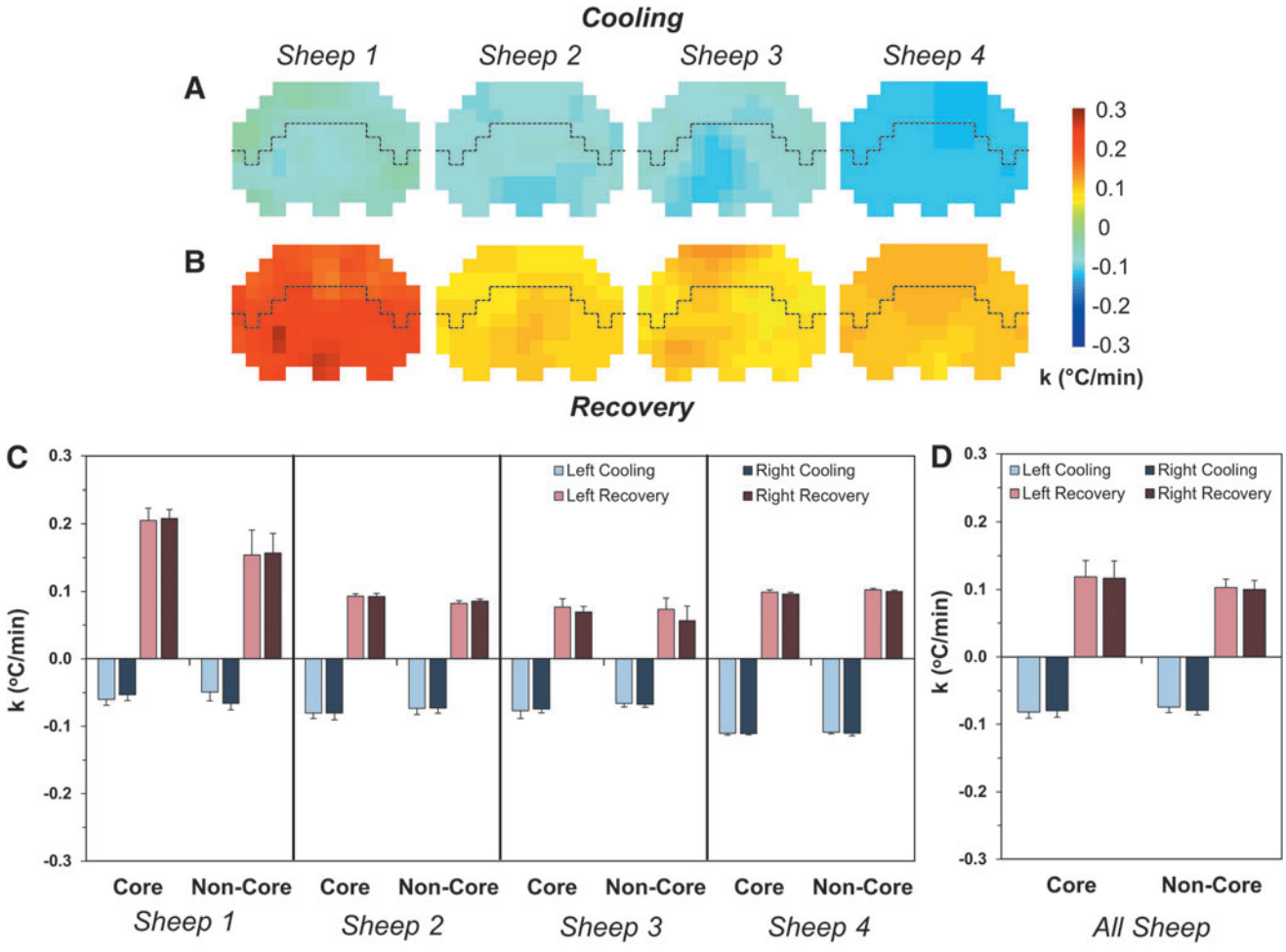

FIG. 5. Rates of temperature change during cooling and recovery in all four sheep. Spatial distributions of the rate of temperature change in an axial slice (slice c in Fig. 1) during the first cooling event using the right catheter (**A**) and during the first recovery (**B**). Quantification of the rate of temperature change during cooling and recovery are shown for both the left and right hemispheres for core and non-core regions of the brain in individual animals (**C**). Average rates of temperature change are reported for all animals (**D**) with no significant differences between the core and non-core regions of the brain or the left and right hemispheres. Rates of temperature changes are all reported as average ± standard deviation. The dashed line in (A) and (B) represents the demarcation between the core (bottom) and non-core (top) regions.

4 (Supplementary Fig. 2) where the lowest temperature reached was 32.8 ± 0.2 °C.

Discussion

Therapeutic hypothermia is neuroprotective; however, previous methods to achieve hypothermia rely on systemic body cooling, resulting in many adverse effects. Although some targeted cooling methods have been proposed, their effects are modest. External cooling devices may only lower brain temperatures by <1°C.[22] Further, measuring the effects of hypothermia is challenging. With systemic body hypothermia, cooling measurements made on the brain surface are not reflective of temperature in deep brain structures. Because metabolism continues in the presence of hypothermia to varying degrees, the temperature throughout a tissue may not be uniform. Therefore, dynamic measurements of spatial temperature distribution made throughout the target tissue are needed.

In this work, we used temperature mapping with an MRSI method (BIRDS) to measure the temperature distribution throughout the brain during cooling as well as after cooling was stopped (recovery). The usage of a CSF-based intraventricular cooling catheter represents an innovative method for brain cooling. In a previous experiment, we demonstrated cooling of the brain with this CSF-based technology.[17] Brain temperatures in that effort were measured by needle-based temperature sensors that were inserted into the brain parenchyma at a depth of 15 mm posterior and anterior to the ventricles. Because those results were site specific and required an additional burr hole for the insertion of the temperature sensor itself, we undertook this current effort to achieve a more comprehensive and less invasive mapping of cooling throughout the brain.

Measuring the cooling rates allows for a dose-response relationship to be established. The amount of cooling (or the ''dose'') is reflective of the flow rate of saline and the effectiveness of heat transfer between the CSF and the cooling solution. The dose-response relationship can be tuned easily using the cooling rates measured with BIRDS. For example, to achieve a temperature decrease of 2°C in a brain region where the measured cooling rate was 0.1°C/min, we need 20 min of cooling. Faster cooling can be achieved, however, with a higher flow rate of the cooling solution.

The procedure used to insert the catheter is similar to that regularly performed by neurosurgeons to safely access the intraventricular region of the brain to relieve intracranial pressure using ventricular access devices placed in the lateral ventricles. These procedures are commonly and safely performed in the neuro intensive care unit (ICU) and, although not without risks, have a history of successful outcomes in the literature.[23] In addition, expanding this procedure to induce therapeutic hypothermia would add significant benefits without increasing risks.

Other methods currently in use to induce hypothermia, such as intravascular infusions of chilled saline/blood, are also invasive and come with their own risks and may be limited in the degree and length of time hypothermia can be maintained. In contrast, using the CSF cooling catheter, hypothermia could be maintained for as long as the catheter is implanted. Catheters used for intracranial pressure monitoring can be left in place for several days. Therefore, our cooling method is well suited for maintaining hypothermia as long as the temperature of the circulated chilled saline is maintained. Moreover, a benefit of the current system is that cooling can be turned off at any point allowing for rapid rewarming, or the flow could be adjusted to maintain specific temperature reductions in the brain.

Although the circulated saline does not enter and is not in direct contact with the CSF, the intraventricular catheter device allows for rapid cooling of the CSF, which then flows throughout the brain, providing generalized cooling via convection. The surface of the brain in contact with the CSF is very large and is increased even further by interactions with the vasculature in perivascular and interstitial spaces.[24] Therefore, by cooling the CSF, we were able to efficiently and uniformly remove the thermal energy from the brain and thus to modify its thermal environment.

This is somewhat similar to the primary means of heat removal from the brain via cerebral blood circulation, where changing the vasodilation results in increased blood flow and more efficient heat removal (whereas vasoconstriction results in heat accumulation).[25] Although the catheters were inserted through the right and left hemispheres of the brain, the positions of both catheters are near the center of the brain (Fig. 1), which may explain the relatively uniform temperature distribution during cooling/recovery in the ipsilateral versus contralateral hemispheres.

The supersaturation of the saline flowing through the intraventricular catheter can lower the water freezing point; thus, the circulating saline has a temperature of -7 to -10°C in the water pump reservoir. One limitation of the current experimental setup, however, is that the non-MR-compatible pump was located ~7 meters away from the magnet bore, allowing the saline to warm up while flowing through the delivery line. Therefore, the temperature of the cooling fluid reaching the animal was warmer than in our previous experiments.[17] Thus, we expect that even greater and faster brain temperature decreases may be achievable inside the magnet, with optimization of the delivery method (for example, using a thermally isolated delivery line). In human application in the neuro ICU, the length of the cooling lines would be minimal and such issues would not pertain.

A historical thermal map of the primate brain previously has been constructed and illustrated temperature differences of 0.3–0.5°C between brain regions, with the highest temperatures seen in the deep regions of the brain.[26] In the case of basal temperature data in the sheep brain, we observed variations between brain regions of up to 0.7°C, in good agreement with previous literature values demonstrated in a sheep brain.[27]

The effects of anatomical site and activity on brain temperature have been reviewed extensively[24]; these studies highlight potential hemispherical differences in temperature, but also demonstrate temperature fluctuations from sleep, arousal, and stimulation. In addition, under anesthesia, there are also differences in brain temperature from the awake state, with temperature reductions seen, and minimal fluctuations in temperature.

We did not observe any interhemispherical differences, with regional differences between the right and left hemisphere generally not exceeding 0.3°C. It has been noted that regional brain temperatures increase more rapidly than arterial temperatures, suggesting that local heat production because of increased metabolism is primarily responsible. In humans, deep brain temperature is less than 1°C higher than body temperature.[28] Ambient environmental temperature can impact superficial cerebral sites, but has no effect on deep brain structures or blood temperature.

Temperature mapping with BIRDS using $TmDOTMA^-$ has been well characterized and validated.[19] In contrast to previous applications of BIRDS for temperature mapping where $TmDOTMA^-$ was injected into circulating blood, here we injected the agent directly into the CSF via the intraventricular cooling catheter. Other temperature mapping techniques, such as phase shift MRI, have been applied to monitor temperature changes in the brain.[14] The phase shift MRI method can only report a change in temperature and not the absolute temperature, however. Further, accuracy is reduced because the sensitivity of the temperature measurement by

phase shift MRI is on the order of 0.01 ppm/°C, compared with 0.7 ppm/°C for BIRDS with $TmDOTMA^-$.

The error in temperature measurement is related directly to the signal-to-noise ratio (SNR) observed for the $-CH_3$ proton resonance.[19] The SNR values higher than five measured in the sheep brain indicate an error in the temperature measurements smaller than 0.01°C. Similar cooling experiments were performed previously in sheep by our group, in which the local temperature was measured using thermocouples in four brain regions. The temperature changes (1.4–5.7°C) and the rates recorded are similar to those observed here with BIRDS.[17]

In terms of changes during cooling seen within individual sheep in this study, the absolute temperature for sheep 4 decreased much more than in the other three sheep. This can be attributed to the baseline temperature being higher by nearly 1°C in this animal. Also, since brain metabolism competes with the cooling process, this higher temperature decrease could be because of a lower brain metabolism in this sheep, possibly due to a deeper state of anesthesia. We also observed that the absolute temperature for sheep 1 and 2 during recovery increased by about 1°C more than in the other two sheep (Fig. 4B, 4C), most likely because of a lower brain temperature at the beginning of the recovery period, achieved while cooling the brain using both catheters (in sheep 3 and 4, only the right catheter was used for cooling before the recovery period).

Although the number of animals used ($n = 4$) was low, the aim of the current study was to assess the degree of hypothermia achieved by intraventricular cooling by measuring 3D temperature profiles throughout the brain. One limitation of this study is that there was no secondary validation of the temperature changes measured with BIRDS. Direct temperature recordings, however, using the same cooling system have been made previously with thermocouple probes inserted directly in four cortical brain locations.[17] These thermocouple measurements provided similar results, with temperature decreases of 3.7°C, which are in agreement with the current BIRDS results from the cortical (non-core) regions of the brain (3.0°C). This comparison is summarized in Supplementary Table 1; see online supplementary material at www.liebertpub.com.

Comparisons between these two measurements, however, must be mindful of the following differences. For the thermocouple measurements, cooling was induced using two catheters (right and left) with continuous cooling for 3 h. For BIRDS, cooling was varied between the right and left catheter (or both) and was stopped and started over the course of 2 h to better study the dynamics of the temperature changes induced by the cooling catheter. Moreover, for the thermocouple measurements, the temperature reported is an average value from four temperature sensors placed in the anterior and posterior cortex of both the right and left hemisphere, while for BIRDS, we used the average cortical temperature. It should also be noted that there is variability between animals for both thermocouple and BIRDS measurements, which may be because of the effectiveness of the catheter placement, the level of brain metabolism, and/or anesthesia depth.

Moreover, the temperature measurements with BIRDS have been validated *in vivo* in the rodent brain under several different activity states.[19,29] The $TmDOTMA^-$ MR signal is not dependent on ion concentrations or pH, which is important for its application to disease states, such as TBI or stroke, which are known to induce both ion imbalances and dysregulated osmoregulation. The measurements made in this current study are performed in otherwise healthy brain tissue, which should have uniform characteristics allowing for quantitative temperature mapping without other contributing factors.

Systemic body temperatures measured by a rectal probe were monitored throughout the duration of this study and showed only minimal changes (± 1°C) in systemic temperature throughout the experiment (Supplementary Fig. 2; see online supplementary material at www.liebertpub.com). Note that, typically, anesthetized animals experience a decrease in body temperature; therefore, while the animals were anesthetized, a body warming blanket was used to maintain the body temperature despite the cooling of the brain tissue. This is an applicable strategy that could be employed clinically, because heat gain by the body is not expected to significantly increase brain temperature, permitting maintenance of systemic normothermia.

Hypothermia is the only treatment shown to be neuroprotective in global cerebral ischemia after circulatory arrest. This provides positive implications for potential neuroprotection in TBI and ischemic stroke. Further, hypothermia has been a mainstay of surgical procedures involving deliberate cardiac arrest, including many forms of open heart surgery (in which core body temperatures are commonly lowered to below 18°C).[30] Although significant hypothermia is required after spontaneous cardiac arrest, the data after ischemic stroke are less clear, with neuroprotective effects being demonstrated with much smaller levels of cooling (e.g., core body temperature reductions to 34°C).[31]

Lowering the temperature results in reduced cellular metabolism and lower oxygen demands of any tissue and reduces the stress placed on damaged cells. The greater the tissue cooling, the greater the reduction in oxygen consumption, and therefore oxygen demand, allowing cells to tolerate inflammatory and ischemic conditions better. There are also affected mechanisms at the cellular level, whereby hypothermia reduces the development of inflammation and necrosis in ischemic regions.

Ischemia leads to neuronal damage through several mechanisms, including energy depletion, excitotoxicity, calcium influx, membrane damage, formation of free radicals, and activation of protein kinases.[31] In the case of TBI, treatment is challenging because of the heterogeneity of the presenting modes of injury and clinical symptoms.[4] Further, the time after injury or the onset of ischemia will always be a confounding factor in understanding the effects of hypothermia.

Although questions will always remain about the optimal cooling methodology, targeted temperature, and duration of hypothermia, selective and targeted cooling strategies show potential for improved management of localized brain injury and ischemia, where temperature mapping with BIRDS could provide the means to assess the efficiency of the cooling strategies throughout the whole brain. In the future, we plan to compare different cooling strategies and to assess therapeutic efficacy of mild hypothermia in a large animal model of TBI.

Conclusion

Recent clinical trials failed to demonstrate the promise of therapeutic hypothermia in TBI, yet neuroprotection against ischemic injury remains a high clinical priority. Despite the myriad of successful animal studies in TBI as well as in other morbidities, use of topical cooling has been unsuccessful. Perhaps it is not the hypothermia itself that has limited the translation of therapeutic hypothermia, however, but rather the method of delivery has not been effective. The use of this novel CSF-based cooling platform results in significant and uniform cooling throughout the cortex of the sheep brain, which has a ventricular landscape similar to the human brain. Interestingly, by using a single catheter, the technique can induce cooling throughout both hemispheres of the brain.

Temperature mapping with high spatiotemporal resolution using BIRDS was feasible in the sheep brain both before and after induction of hypothermia. BIRDS allows for rapid imaging that has high temperature sensitivity, allowing for robust and accurate

temperature mapping. In these experiments, CSF-based cooling provides a very efficient method for inducing therapeutic hypothermia, raising promise for improved clinical management of TBI or ischemia, because the brain can be cooled selectively, obviating the adverse side effects of whole body cooling.

Acknowlegments

This work was supported in part by NSF (STTR 0923928) and NIH (R01 EB023366, R01 EB011968, R01 CA140102, P30 NS052519, T32 GM007205).

Author Disclosure Statement

John W. Simmons is the CEO of CoolSpine, LLC (Woodbury, CT). John A. Elefteriades is a cofounder of CoolSpine, LLC, consultant at CryoLife and Dura Biotech, and on the data and safety monitoring boards of Jarvik Heart and Terumo. For all other authors, no competing financial interests exist.

Supplementary Material

Supplementary Table S1
Supplementary Figure S1
Supplementary Figure S2
Supplementary Figure S3
Supplementary Figure S4

References

1. Cooper, D.J., Nichol, A.D., Bailey, M., Bernard, S., Cameron, P.A., Pili-Floury, S., Forbes, A., Gantner, D., Higgins, A.M., Huet, O., Kasza, J., Murray, L., Newby, L., Presneill, J.J., Rashford, S., Rosenfeld, J.V., Stephenson, M., Vallance, S., Varma, D., Webb, S.A., Trapani, T., McArthur, C., POLAR Trial Investigators and the ANZICS Clinical Trials Group. (2018). Effect of early sustained prophylactic hypothermia on neurologic outcomes among patients with severe traumatic brain injury: The POLAR Randomized Clinical Trial. JAMA 320, 2211–2220.
2. Cooper, D.J., Nichol, A., and Presneill, J. (2016). Hypothermia for intracranial hypertension after traumatic brain injury. N. Engl. J. Med. 374, 1384.
3. Mrozek, S., Vardon, F., and Geeraerts, T. (2012). Brain temperature: physiology and pathophysiology after brain injury. Anesthesiol. Res. Pract. 2012, 989487.
4. Blennow, K., Brody, D.L., Kochanek, P.M., Levin, H., McKee, A., Ribbers, G.M., Yaffe, K., and Zetterberg, H. (2016). Traumatic brain injuries. Nat. Rev. Dis. Primers 2, 16084.
5. Dietrich, W.D. and Bramlett, H.M. (2010). The evidence for hypothermia as a neuroprotectant in traumatic brain injury. Neurotherapeutics 7, 43–50.
6. Childs, C. and Lunn, K.W. (2013). Clinical review: Brain-body temperature differences in adults with severe traumatic brain injury. Crit. Care 17, 222.
7. Erickson, K.M. and Lanier, W.L. (2003). Anesthetic technique influences brain temperature, independently of core temperature, during craniotomy in cats. Anesth. Analg. 96, 1460–1466.
8. Wass, C.T., Cable, D.G., Schaff, H.V., and Lanier, W.L. (1998). Anesthetic technique influences brain temperature during cardiopulmonary bypass in dogs. Ann. Thorac. Surg. 65, 454–460.
9. Karaszewski, B., Wardlaw, J.M., Marshall, I., Cvoro, V., Wartolowska, K., Haga, K., Armitage, P.A., Bastin, M.E., and Dennis, M.S. (2006). Measurement of brain temperature with magnetic resonance spectroscopy in acute ischemic stroke. Ann. Neurol. 60, 438–446.
10. Michenfelder, J.D. and Milde, J.H. (1991). The relationship among canine brain temperature, metabolism, and function during hypothermia. Anesthesiology 75, 130–136.
11. Soleimanpour, H., Rahmani, F., Golzari, S.E., and Safari, S. (2014). Main complications of mild induced hypothermia after cardiac arrest: a review article. J. Cardiovasc. Thorac. Res. 6, 1–8.
12. Christian, E., Zada, G., Sung, G., and Giannotta, S.L. (2008). A review of selective hypothermia in the management of traumatic brain injury. Neurosurg. Focus 25, E9.
13. Straus, D., Prasad, V., and Munoz, L. (2011). Selective therapeutic hypothermia: a review of invasive and noninvasive techniques. Arq. Neuropsiquiatr. 69, 981–987.
14. Sedlacik, J., Kjørstad, Å., Nagy, Z., Buhk, J.H., Behem, C.R., Trepte, C.J., Fiehler, J., and Temme, F. (2018). Feasibility study of a novel high-flow cold air cooling protocol of the porcine brain using MRI temperature mapping. Ther. Hypothermia Temp. Manag. 8, 45–52.
15. Takeda, Y., Hashimoto, H., Fumoto, K., Danura, T., Naito, H., Morimoto, N., Katayama, H., Fushimi, S., Matsukawa, A., Ohtsuka, A., and Morita, K. (2012). Effects of pharyngeal cooling on brain temperature in primates and humans: a study for proof of principle. Anesthesiology 117, 117–125.
16. Wu, C., Zhao, W., An, H., Wu, L., Chen, J., Hussain, M., Ding, Y., Li, C., Wei, W., Duan, J., Wang, C., Yang, Q., Wu, D., Liu, L., and Ji, X. (2018). Safety, feasibility, and potential efficacy of intraarterial selective cooling infusion for stroke patients treated with mechanical thrombectomy. J. Cereb. Blood Flow Metab. 38, 2251–2260.
17. Moomiaie, R.M., Gould, G., Solomon, D., Simmons, J., Kim, J., Botta, D., and Elefteriades, J.A. (2012). Novel intracranial brain cooling catheter to mitigate brain injuries. J. Neurointerv. Surg. 4, 130–133.
18. Coman, D., Trubel, H.K., Rycyna, R.E., and Hyder, F. (2009). Brain temperature and pH measured by (1)H chemical shift imaging of a thulium agent. NMR Biomed. 22, 229–239.
19. Coman, D., Trubel, H.K., and Hyder, F. (2010). Brain temperature by Biosensor Imaging of Redundant Deviation in Shifts (BIRDS): comparison between TmDOTP5- and TmDOTMA-. NMR Biomed. 23, 277–285.
20. Coman, D., de Graaf, R.A., Rothman, D.L., and Hyder, F. (2013). In vivo three-dimensional molecular imaging with Biosensor Imaging of Redundant Deviation in Shifts (BIRDS) at high spatiotemporal resolution. NMR Biomed. 26, 1589–1595.
21. Ella, A., Delgadillo, J.A., Chemineau, P., and Keller, M. (2017). Computation of a high-resolution MRI 3D stereotaxic atlas of the sheep brain. J. Comp. Neurol. 525, 676–692.
22. Curran, E.J., Wolfson, D.L., Watts, R., and Freeman, K. (2017). Cold blooded: evaluating brain temperature by MRI during surface cooling of human subjects. Neurocrit. Care 27, 214–219.
23. Hawthorne, C., and Piper, I. (2014). Monitoring of intracranial pressure in patients with traumatic brain injury. Front. Neurol. 5, 121.
24. Wang, H., Wang, B., Normoyle, K.P., Jackson, K., Spitler, K., Sharrock, M.F., Miller, C.M., Best, C., Llano, D., and Du, R. (2014). Brain temperature and its fundamental properties: a review for clinical neuroscientists. Front. Neurosci. 8, 307.
25. Blowers, S., Marshall, I., Thrippleton, M., Andrews, P., Harris, B., Bethune, I., and Valluri, P. (2018). How does blood regulate cerebral temperatures during hypothermia? Sci. Rep. 8, 7877.
26. Hayward, J.N., and Baker, M.A. (1968). Role of cerebral arterial blood in the regulation of brain temperature in the monkey. Am. J. Physiol. 215, 389–403.
27. Hemingway, A., Robinson, R., Hemingway, C., and Wall, J. (1966). Cutaneous and brain temperatures related to respiratory metabolism of the sheep. J. Appl. Physiol. 21, 1223–1227.
28. Bertolizio, G., Mason, L., and Bissonnette, B. (2011). Brain temperature: heat production, elimination and clinical relevance. Paediatr. Anaesth. 21, 347–358.
29. Coman, D., Sanganahalli, B.G., Jiang, L., Hyder, F., and Behar, K.L. (2015). Distribution of temperature changes and neurovascular coupling in rat brain following 3,4-methylenedioxymethamphetamine (MDMA, ''ecstasy'') exposure. NMR Biomed .28, 1257–1266.
30. Saad, H., and Aladawy, M. (2013). Temperature management in cardiac surgery. Glob. Cardiol. Sci. Pract. 2013, 44–62.
31. Wu, T.C. and Grotta, J.C. (2013). Hypothermia for acute ischaemic stroke. Lancet Neurol. 12, 275–284.

Address correspondence to:
Daniel Coman, PhD
Department of Radiology and Biomedical Imaging
Yale University
300 Cedar Street, TAC N144
New Haven, CT 06519

E-mail: daniel.coman@yale.edu